Spacetime geometries and light trapping in travelling refractive index perturbations



2010 New J. Phys. 12 095021

(http://iopscience.iop.org/1367-2630/12/9/095021)

New Journal of Physics
The open-access journal for physics

# Spacetime geometries and light trapping in travelling refractive index perturbations

**S L Cacciatori[1,2,6], F Belgiorno[3], V Gorini[1,2], G Ortenzi[4], L Rizzi[1], V G Sala[1] and D Faccio[5]**

[1] Department of Physics and Mathematics, Università dell'Insubria, Via Valleggio 11, IT-22100 Como, Italy
[2] INFN sezione di Milano, via Celoria 16, IT-20133 Milano, Italy
[3] Dipartimento di Fisica, Università di Milano, Via Celoria 16, IT-20133 Milano, Italy
[4] Dipartimento di Matematica e Applicazioni, Università degli Studi di Milano, Bicocca, IT-20125 Milano, Italy
[5] CNISM and Department of Physics and Mathematics, Università dell'Insubria, Via Valleggio 11, IT-22100 Como, Italy
E-mail: sergio.cacciatori@uninsubria.it

*New Journal of Physics* **12** (2010) 095021 (14pp)
Received 30 April 2010
Published 30 September 2010
Online at http://www.njp.org/
doi:10.1088/1367-2630/12/9/095021

**Abstract.** In the framework of transformation optics, we show that the propagation of a locally superluminal refractive index perturbation (RIP) in a Kerr medium can be described, in the eikonal approximation, by means of a stationary metric, which we prove to be of Gordon type. Under suitable hypotheses on the RIP, we obtain a stationary but not static metric, which is characterized by an ergosphere and by a peculiar behaviour of the geodesics, which are studied numerically, also accounting for material dispersion. Finally, the equation to be satisfied by an event horizon is also displayed and briefly discussed.

[6] Author to whom any correspondence should be addressed.

**Contents**



## 1. Introduction

Effective geometries for light, first introduced by Gordon [1] and then extended to nonlinear electrodynamics, are able to provide analogue black hole metrics and also the possibility of performing experiments involving Hawking analogue radiation [2]–[14]. Recently, Philbin *et al* [15] proposed an optical analogue in which a soliton with intensity $I$, propagating in an optical fibre, generates through the nonlinear Kerr effect a refractive index perturbation (RIP), $\delta n = n_2 I$, where $n_2$ is the Kerr index. The same mechanism has also been generalized to a full four-dimensional (4D) geometry by Faccio *et al* [16]. The RIP modifies the spacetime geometry as seen by co-propagating light rays and, similarly to the acoustic analogy, if the RIP is locally superluminal, i.e. if it travels faster than the phase velocity of light in the medium, a trapping horizon is formed and Hawking radiation is to be expected. A full analysis for the case of a static black hole metric has been recently discussed in [17]. Our aim here is to tackle the following aspects: (i) provide a general derivation of the metric in the eikonal approximation from relativistic nonlinear electrodynamics in a medium and (ii) perform a first analysis for a generic RIP that gives rise to a stationary (but in general non-static) metric. The metric we obtain allows us to determine in a straightforward way the limits under which an ergoregion occurs. Then a study of the behaviour of null geodesics follows, with the aim of identifying conditions such that trapping of light occurs inside the dielectric perturbation. Finally, the equation to be satisfied by an event horizon is provided.

## 2. Effective geometry

In this section, we introduce the specific analogue model that we have analysed. As we need to work both in the laboratory frame and in an inertial reference frame that is moving at relativistic speed with respect to the original frame, it is convenient to adopt a covariant formalism. Then, consider a reference frame in which the dielectric medium is moving with four-velocity $u^\mu$. Moreover, consider a medium for which the permittivity and permeability have, respectively, the form

$$\epsilon^{\alpha\beta} = \varepsilon(E)(\eta^{\alpha\beta} - u^\alpha u^\beta), \tag{1}$$

$$\mu^{\alpha\beta} = \mu_0 \mu_r (\eta^{\alpha\beta} - u^\alpha u^\beta), \tag{2}$$

where $\eta_{\mu\nu}$ is the Minkowski metric tensor. That is, the permittivity is a function of the invariant electric field amplitude $E := \sqrt{-E^\mu E_\mu}$ alone. In the laboratory frame, this reduces to the assumption that a polarization is induced in the medium only when it is exposed to an electric field and that the nonlinear effects depend only on the intensity of the latter. The permeability is assumed to be constant and equal to the product $\mu$ of the vacuum permeability $\mu_0$ and the relative permeability $\mu_\mathrm{r}$ of the medium. These conditions indeed hold true for diverse nonlinear media. For example, for the case of an isotropic $\chi^{(3)}$ medium, in the laboratory frame

$$\varepsilon = \varepsilon_0 \varepsilon_\mathrm{r} = \varepsilon_0 (1 + \chi^{(1)} + \chi^{(3)} E^2), \tag{3}$$

where $\varepsilon_0$ is the vacuum permittivity.

Nonlinear effects are usually very small and a very strong field is needed to exploit the nonlinearity of the medium itself. Thus, we assume that there exists a strong, background field $E$, which fixes the properties of the dielectric. Note that these assumptions are rather general. In fact, equations (1) and (2) hold for any nonlinear, homogeneous dielectric, no matter how the strong background pulse is generated [6]. We are interested in the small and rapidly oscillating fluctuations of the electromagnetic field on top of such a background[7].

According to the results of [6, 11, 12], these small fluctuations 'feel' an effective curved spacetime. The result is what a relativist would call a 'bi-metric' theory. In other words, there exist two classes of rays, namely ordinary and extraordinary rays, which correspond to two different polarizations of the background field. This phenomenon is analogous to birefringence in uni-axial crystals, where the ordinary and extraordinary rays each obey distinct quadratic dispersion relations. In the analogue gravity terminology, each ray 'feels' a different geometry, or *analogue metric*: the Gordon's metric

$$g^{(+)}_{\mu\nu} = \eta_{\mu\nu} - u_\mu u_\nu \left[1 - \frac{1}{n^2}\right] \tag{4}$$

for the ordinary rays and the metric

$$g^{(-)}_{\mu\nu} = \eta_{\mu\nu} - u_\mu u_\nu \left[1 - \frac{1}{n^2(1+\xi)}\right] + \frac{\xi}{\xi+1} l_\mu l_\nu \tag{5}$$

for the extraordinary rays. In (4)–(5), we have introduced the 'nonlinear parameter' $\xi := \frac{E}{\varepsilon}\frac{\mathrm{d}\varepsilon}{\mathrm{d}E}$, the background field polarization four-vector $l_\mu := \frac{E_\mu}{E}$, and the refractive index $n := \sqrt{\varepsilon_\mathrm{r}\mu_\mathrm{r}}$. In the Cartesian coordinates $(t, x, y, z)$, $\eta_{\mu\nu} = \mathrm{diag}(c^2, -1, -1, -1)$.

In the appendix, we show that, under reasonable approximations, the extraordinary metric is equivalent to the Gordon one, albeit with a different effective Kerr perturbation of the refractive index, i.e. $n = n_0 + 3dn$ instead of $n = n_0 + dn$. Thus, we restrict our attention to the Gordon metric.

In the following, we study the light-like geodesics of the analogue metrics. It is important to note that these geodesics describe the spacetime trajectories of monochromatic waves. In the present paper, we often refer to these trajectories with the term 'light rays'. However, these should not be confused with the usual light rays referred to in geometrical optics which, in the Newtonian picture, describe the trajectories of wave packets (or 'photons'). For this reason, in the forthcoming sections, we analyse the monochromatic components (congruences of light-like

[7] For reasons connected with the actual experimental verification of this theoretical framework, we may think of this strong background field as a spatially localized (albeit rather extended) pulse, which is travelling through the medium.

geodesics) of the electromagnetic field and the analogue geodesic motion of the related constant phase surfaces, which are precisely the objects involved in the study of the analogue Hawking radiation [18, 19]. By contrast, we do not consider the notion of the 'photon' (or wave packet) here.

## 3. The metric in the refractive index perturbation (RIP) frame

Consider the case of a pulse moving with uniform velocity $v$ along the positive $x$-axis. According to the above discussion, the pulse excites a localized RIP which also moves accordingly. The latter can then be analytically described as a function of $x - vt$ and, assuming cylindrical symmetry, of the transversal coordinate $\rho = \sqrt{y^2 + z^2}$. Thus, in the laboratory frame, $n = n_0 + \delta n(x - vt, \rho)$. In this situation, it is convenient to express the Gordon metric in a reference frame which is co-moving with the RIP itself:

$$\begin{aligned} \mathrm{d}s^2 = c^2\gamma^2\frac{1}{n^2}\left(1+\frac{nv}{c}\right)\left(1-\frac{nv}{c}\right)\mathrm{d}t'^2 + 2\gamma^2\frac{v}{n^2}\left(1-n^2\right)\mathrm{d}t'\mathrm{d}x' \\ -\gamma^2\left(1+\frac{v}{nc}\right)\left(1-\frac{v}{nc}\right)\mathrm{d}x'^2 - \mathrm{d}\rho^2 - \rho^2\,\mathrm{d}\phi^2, \end{aligned} \tag{6}$$

where the primed coordinates are relative to the co-moving frame, and

$$n := n_0 + \delta n(x', \rho). \tag{7}$$

Here, $\delta n$ is a $C^\infty$ function, rapidly decaying at infinity and with a single maximum of height $\eta$, describing the RIP. It is then evident that both $\partial_{t'}$ and $\partial_\phi$ are Killing vectors for the given class of metrics. Any specific choice for the function $\delta n$ gives rise to a specific metric in the aforementioned class. We point out that an isotropic refractive index in the laboratory frame corresponds to an anisotropic refractive index in the pulse frame due to length contraction associated with a boost in the $x$-direction. If the refractive index depends explicitly on $\rho$, the metric is stationary but not static: the integrability conditions stated in the Frobenius theorem [20] are not satisfied. In particular, if $\xi_\mu = (g_{00}, g_{01}, 0, 0)$ are the covariant components of the time-like Killing vector $\partial_{t'}$, the integrability conditions $\xi_{[\lambda}\nabla_\mu\xi_{\nu]} = 0$, for $\lambda = 0$, $\mu = 1$ give $\xi_0(\nabla_1\xi_\nu - \nabla_\nu\xi_1) + \xi_1(\nabla_\nu\xi_0 - \nabla_0\xi_\nu) = 0$, i.e. for $\nu = \rho$, $g_{00}(-\partial_\rho g_{01}) + g_{01}\partial_\rho g_{00} = 0$, which is easily seen to be not satisfied. The static case is obtained if $\delta n$ does not depend on $\rho$, and it has been extensively studied in [17]. Here, we consider the more general stationary, non-static case[8]. We first point out that for our class of metrics an ergosurface is allowed, given by the locus of points satisfying the equation

$$g_{00} = 0 \Leftrightarrow 1 - \frac{nv}{c} = 0. \tag{8}$$

This equation admits solutions only for the range of RIP velocities $v$ given by

$$\frac{1}{n_0+\eta} \leqslant \frac{v}{c} < \frac{1}{n_0}. \tag{9}$$

[8] A simple, non-technical definition of static and stationary spacetimes can be given as follows. A spacetime is stationary if it is possible to find a reference frame in which the metric coefficients do not depend on time. This means that time translation is a symmetry of the spacetime. However, such a spacetime might not be invariant under time reversal. In the case of time-reversal invariance, the spacetime is not only stationary but also static. An example of static spacetime is the Schwarzschild solution, describing the static empty spacetime outside a non-rotating black hole. If the black hole has a non-vanishing angular momentum the spacetime is still invariant under time translations; however, time reversal reverses the sign of the angular momentum, turning a clockwise spinning black hole to an anticlockwise one. Then, the spacetime around a spinning black hole is stationary, but not static.

At the ergosurface, which is the boundary of the ergoregion, the Killing vector $\partial_{t'}$ vanishes, and on entering the ergoregion it changes sign. Here, in contrast with the static case, the ergosurface does not coincide with the event horizon. Indeed, the given hypersurface is not a light-like one, as can be easily verified by looking at the behaviour of its normal vector. However, for $\rho = 0$ it actually becomes light-like, i.e. it meets the event horizon in the antipodal points which solve

$$\delta n(x', 0) = \frac{c - n_0 v}{v}. \tag{10}$$

For stationary non-static situations, it is more difficult to identify a non-trivial event horizon in effective geometries (see e.g. Visser's analysis for the case of acoustic black holes [21]). Before discussing the question of the existence of an event horizon, we investigate whether the path of light rays, that is, the null geodesic curves of metric (6), do suggest the existence of such a horizon.

## 4. Geodesics and trapping of light

In the laboratory frame, the metric (6) is

$$\mathrm{d}s^2 = \frac{c^2}{n^2(x - vt, y, z)}\mathrm{d}t^2 - \mathrm{d}x^2 - \mathrm{d}y^2 - \mathrm{d}z^2. \tag{11}$$

We model the RIP with a Gaussian-shaped function that propagates along the $x$-axis with velocity $v$. We also suppose that, during the propagation, it keeps its shape both in space and in time. Assuming cylindrical symmetry, we need to account only for one of the two transverse coordinates, say, $y$. Then, we write the refractive index in the form

$$n = n_0 + \delta n, \quad \delta n = \eta \mathrm{e}^{[-y^2-(x-vt)^2]/\sigma^2}. \tag{12}$$

Thus, the geodesic equations for null rays take the explicit form

$$\ddot{x} = -\frac{2}{\sigma^2}\frac{\delta n}{n^3}(x - vt)c^2\dot{t}^2, \tag{13}$$

$$\ddot{y} = -\frac{2}{\sigma^2}\frac{\delta n}{n^3}yc^2\dot{t}^2, \tag{14}$$

$$\ddot{t} = \frac{2}{\sigma^2}\left[\frac{\delta n}{n^2}v(x - vt)\dot{t}^2 - y\dot{y}\dot{t} - (x - vt)\dot{x}\dot{t}\right], \tag{15}$$

where the dot denotes derivation w.r.t. an affine parameter $\lambda$. A trivial solution is $\frac{\mathrm{d}x}{\mathrm{d}t} = c/n$, $y(t) = 0$. However, in the general case a numerical analysis is required. In the following subsection, we solve the equations above using Matlab's ode45 function. This analysis will provide an insight into the underlying physics.

### *4.1. Numerical solutions and trapping of light*

Along a geodesic we have $(c\dot{t}, \dot{x}, \dot{y}, \dot{z}) = (k^0, k^1, k^2, k^3) = (n^2\omega/c, k_x, k_y, k_z)$, and taking the first derivative (with respect to the affine parameter $\lambda$) of the relation $c\dot{t} = n^2\omega/c$, we find an equation for $\dot{\omega}$ that determines the evolution of the frequency of the ray along a geodesic. At this point a comment is in order: here we have defined $\omega$ as the zeroth covariant component of the four-momentum $k^\mu$. It is easy to see that this corresponds to measuring frequencies as the inverse

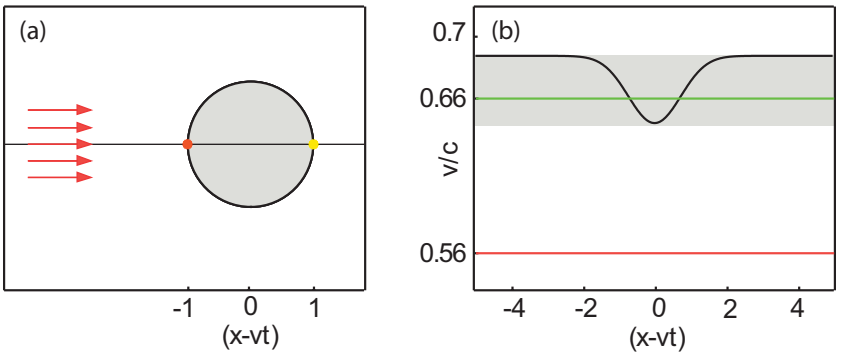


**Figure 1.** (a) Sketch showing the initial conditions of the simulation. (b) Light ray phase velocity $(c/n)$. The shaded region highlights the range of velocities of the RIP for which the rays are trapped. The two straight lines indicate the values of $v/c$ used in the simulations.

of the lapse of coordinate time between two successive crests (this time is the Minkowskian time measured by the laboratory observer). This is of course different from the analogue proper time $\mathrm{d}\tau = \mathrm{d}s/c$ of the analogue metric (11), which has no physical significance: experimental measurements refer to the true Minkowski metric and not to the analogue curved metric.

Then, for the evolution of the frequency $\omega$ along the path of the ray, we obtain

$$\dot{\omega} = \frac{\ddot{t} - 2\omega n \dot{\delta} n}{n^2}. \tag{16}$$

For the sake of definiteness assume the propagation to be in fused silica and the rays to have initial wavelength $\lambda_{\mathrm{in}} = 527\,\mathrm{nm}$. We assume the RIP to have $\sigma = 1\,\mathrm{m}$ and amplitude $\eta = 0.1$, which is quite an unrealistic situation, but simple to deal with. Indeed, the aim of the simulation is merely to study the qualitative behaviour of the geodesics. We have verified that this behaviour does not change, even for much smaller and realistic values of $\sigma \sim 1$–$100\,\mu\mathrm{m}$.

The other parameters of the simulation are the velocity $v$ of the RIP and the initial conditions of the rays, i.e. the array $\{t_{\mathrm{in}}, x_{\mathrm{in}}, y_{\mathrm{in}}, \dot{t}_{\mathrm{in}}, \dot{x}_{\mathrm{in}}, \dot{y}_{\mathrm{in}}\}$. In the simulation, the rays start away from the RIP (which is right moving) and their initial velocity is directed along the $x$-axis, as shown in the sketch of figure 1(a). More precisely, the initial conditions are $\{0, x_{\mathrm{in}}, y_{\mathrm{in}}, \dot{t}_{\mathrm{in}}, \dot{x}_{\mathrm{in}}, 0\}$, with the additional constraints $\dot{x}_{\mathrm{in}}/\dot{t}_{\mathrm{in}} = c/n_0$ and $c\dot{t}_{\mathrm{in}} = n_0^2\omega_{\mathrm{in}}$.

The results of the simulation show that the behaviour of null geodesics is strongly dependent on the velocity $v$ of the RIP. Namely, there exists a range of velocities for which the rays are trapped[9], and these coincide with those predicted by equation (9) (shaded region in figure 1(b)). On the other hand, for lower values of $v$, the rays that enter the RIP are bent and eventually escape. In figure 1(b), the black curve represents the velocity of an axial ray, i.e. of a ray propagating along the $x$-axis, versus $x - vt$. In the same figure, we represent with horizontal lines two choices for the RIP velocity, representing two possible situations: a faster (green line) one and a slower (red line) one. In the first case (faster RIP), the green line intersects the black curve. As the ray approaches the point corresponding to the first intersection, it slows down due to the increasing refractive index, until it acquires the same velocity of the RIP. Asymptotically, the ray is 'trapped' and moves together with the RIP. In the other case (slower RIP), the ray

[9] This is true also when taking into account the material dispersion, which is neglected in this subsection.

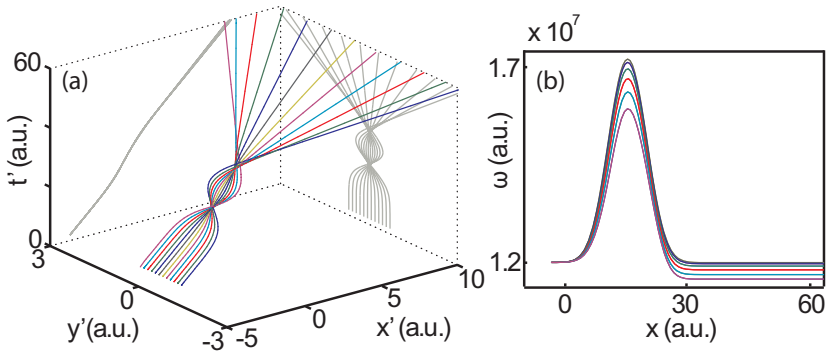


**Figure 2.** Numerical results in the co-moving reference frame (a) and frequency evolution in the laboratory reference frame (b) for the subluminal case.

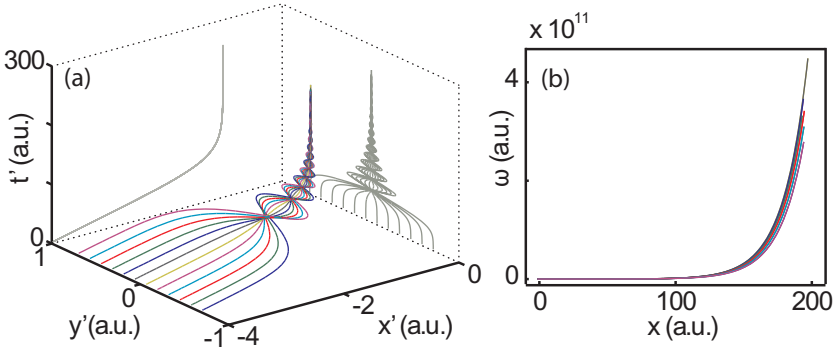


**Figure 3.** Numerical results in the co-moving reference frame (a) and frequency evolution in the laboratory reference frame (b) for the trapping case.

velocity is always larger than the RIP's velocity (red line of figure 1(b)). Then, the ray can cross the RIP and escape. In this 'subluminal' case, no trapping occurs.

*4.1.1. Subluminal RIP.* The RIP propagates at $v = 0.56c$ (red line in figure 1(b)), and it is always slower than the light rays. In figure 2(a) we show the numerical results of the simulation in the co-moving reference frame. The rays start on the left of the RIP. They propagate along straight lines with velocity $c/n_0$ until they reach the RIP. Then, inside the RIP, they slow down, bend and finally escape from the RIP, propagating along straight lines in different directions, depending on their impact parameter $y_{\text{in}}$. The projection of the trajectory on the $(t', x')$ plane, which is also shown figure 2(a), evidently shows a change of slope corresponding to the trajectory being inside the RIP. This means that the rays, while crossing the RIP, slow down. Figure 2(b) represents the evolution of $\omega$ along the $x$-direction in the laboratory reference frame. We observe that, as expected, the frequency varies consistently when the rays reach the RIP. The rays go through a blueshift inside the RIP and then they emerge with a Doppler redshift, due to the fact that the rays are bent and thus emerge at different angles. This behaviour is described in more detail in [16].

*4.1.2. Trapping RIP.* The RIP propagates at $v = 0.66c$ (green line in figure 1(b)). In figure 3(a) we show the numerical results in the co-moving reference frame. The rays propagate initially along straight lines with velocity $c/n_0$ (for clarity, we recall that rays propagate along geodesics

with the *phase* velocity of the corresponding electromagnetic field). When they reach the RIP, they are bent and at the same time slow down. As shown in figure 1(b), at a certain point, away from the centre of the RIP, the rays will have exactly the same velocity as the RIP, and can no longer escape from it. In the co-moving reference frame, they continuously slow down and at the same time they oscillate in the transverse direction with decreasing amplitude oscillations, until, asymptotically, all of them stop at the same point. This point, represented in red in figure 1(a), is the white hole horizon $x_-$ (see the next section). If we look at the slope of the projection $t' = t'(x')$ we see that it diverges, which means that the rays velocity tends to zero corresponding to this point. Clearly, in the laboratory reference frame the rays do not stop, but they move together with the RIP. As shown in figure 3(b), as the rays reach the RIP, their frequency starts growing indefinitely, so we have an infinite blueshift.

### 4.2. *Effects of dispersion*

In the above considerations, we did not account for the material dispersion, that is, we assumed $n(\mathbf{r}, t)$ independent of $\omega$. However, the refractive index of a medium is in general a complicated function of the frequency $\omega$ of the incident wave, that is, $n = n(\mathbf{r}, t, \omega)$. We restrict our attention to the case of 'normal dispersion', that is, we assume that the refraction index grows with frequency. In this case, the full dependence of the refractive index from $\omega$ is phenomenologically described by the Sellmeier equation. A standard way of treating dispersion is to expand $n(\omega)$ in power series of $\omega$ (about an initial frequency $\omega_0$), or equivalently, by the relation $ck = \omega n$, to expand $k$ in power series of $\omega$ as follows:

$$n(\omega) = \frac{c}{\omega}\left(k(\omega_0) + \sum_{n=1}^{\infty} \frac{1}{n!}\frac{\mathrm{d}^n k}{\mathrm{d}\omega^n}\bigg|_{\omega_0} \Delta\omega^n\right). \tag{17}$$

The material dispersion also affects the metric, which therefore depends on the frequency:

$$\mathrm{d}s^2 = \frac{c^2}{n^2(\mathbf{r}, t, \omega)}\mathrm{d}t^2 - \mathrm{d}\mathbf{r}^2. \tag{18}$$

Therefore, different rays propagating in the medium 'feel' different metrics, depending on their frequency. Moreover, even a single ray will see an evolving metric while travelling, since its frequency (and hence the effective metric) changes during the propagation. The geodesic equations (13)–(15) keep the same form as in the non-dispersive case, while equation (16) now takes the form

$$\dot{\omega} = \frac{c^2\ddot{t} - 2\omega n\dot{\delta}n}{n(n + 2\omega \mathrm{d}n_0/\mathrm{d}\omega)}. \tag{19}$$

We highlight that, contrary to the non-dispersive case, the evolution of the geodesics depends on the change in frequency of the ray, owing to the explicit dependence on $\omega$ in the geodesic equations. In the case of a subluminal RIP, dispersion does not modify the qualitative behaviour of the light ray, which remains very similar to the dispersionless case shown in figure 2. On the other hand, for a trapping RIP, the presence of dispersion modifies substantially the geodesics. The results of the numerical simulation are shown in figure 4. The trapping feature of the horizon is still evident. However, taking dispersion into account, the rays are no longer indefinitely trapped inside the RIP and eventually escape. This behaviour is clearly depicted in figure 4(a), where the results are shown in the co-moving reference frame. Note that, at the beginning, the (phase) velocity of the rays is positive, which means that the rays are faster than the RIP, but

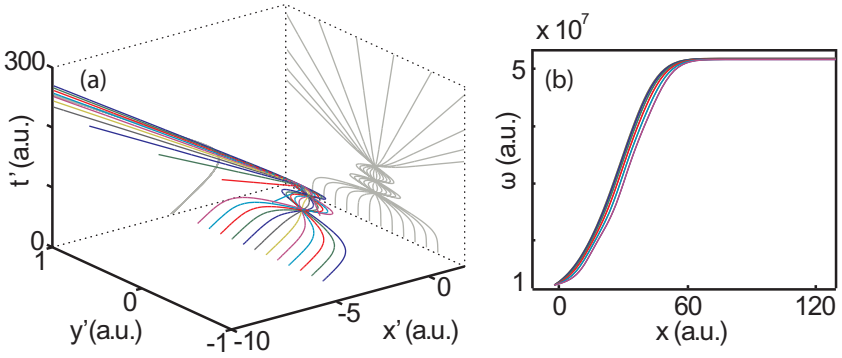


**Figure 4.** Numerical results in the co-moving reference frame (a) and frequency evolution in the laboratory reference frame (b) for the trapping case when we account for dispersion.

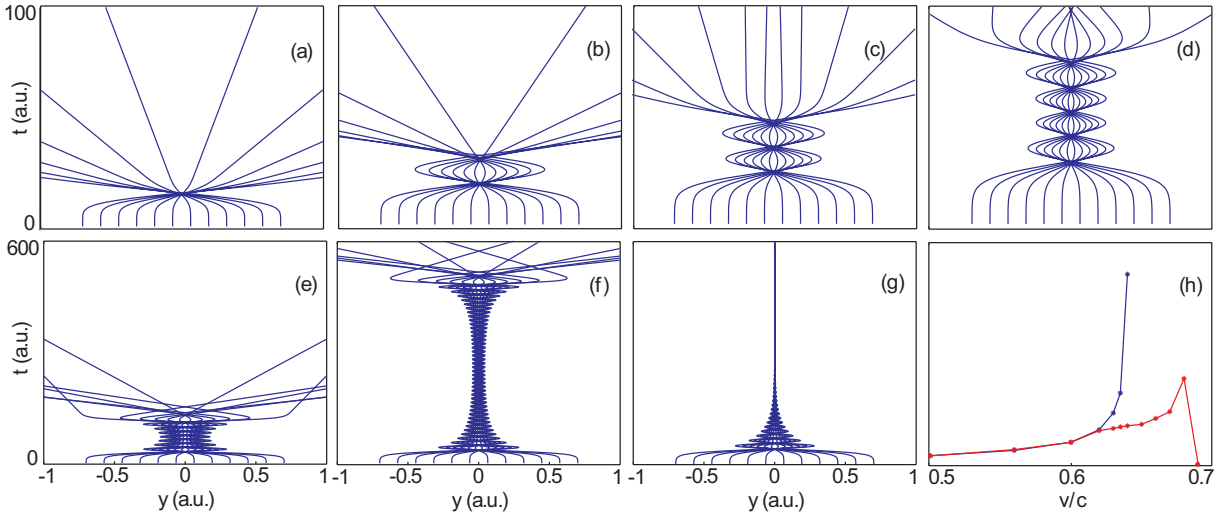


**Figure 5.** (a)–(g) The trapping dynamics in the absence of dispersion for different RIP velocities: (a) $v = 0.5$, (b) $v = 0.56$, (c) $v = 0.6$, (d) $v = 0.62$, (e) $v = 0.63$, (f) $v = 0.64$ and (g) $v = 0.65$. (h) The interaction time versus the velocity of the RIP in the case of no dispersion (blue curve) and in the case of dispersion (red curve).

then it becomes negative, implying that the rays have become slower than the RIP. Let us clarify this aspect. The phase velocity of a ray is defined as $v_r = \omega/k$. Under conditions of normal dispersion, i.e. $\frac{d^2k}{d\omega^2} > 0$, as in our case, $k$ grows faster than linearly with $\omega$ (while without dispersion it would have a linear growth). When the rays approach the RIP, their frequency grows and, at the same time, their phase velocity decreases. Thus, the rays will begin to lag behind with respect to the RIP. When they are out of the RIP they will keep their final frequency. In figure 4(b), we show that the frequency grows only by a finite amount. Therefore, the rays leave the RIP with a finite (albeit very large) blueshift.

*4.2.1. Trapping time.* By increasing the velocity of the RIP from $v = 0.5c$ to $v = 0.65c$ (i.e. approaching the trapping case), the rays spend more and more time inside the RIP. In figure 5(a)–(g), we show this behaviour for different velocities, in the dispersionless case.

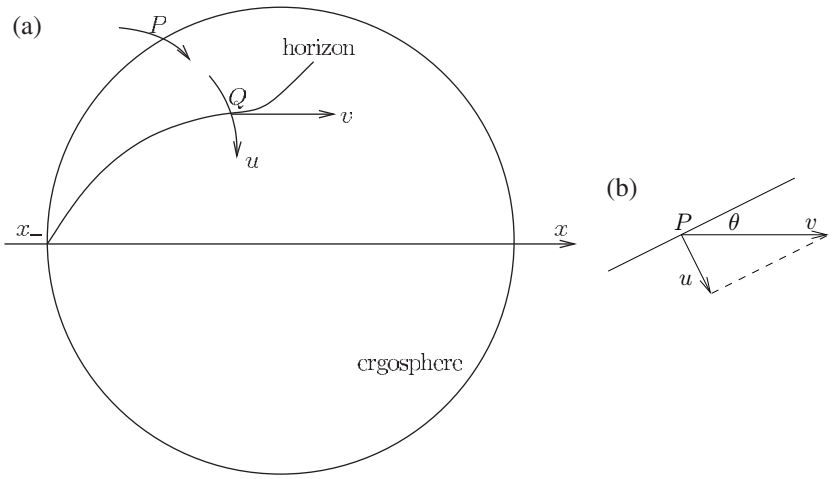


**Figure 6.** (a) Picture of the ergosphere and of the hypothetical horizon at a fixed point of time in the laboratory frame. The small segments at $P$ and $Q$ represent infinitesimal portions of null geodesics (light rays) passing, respectively, through $P$ and $Q$ at that given point of time. (b) Normal velocity $u$ compared to the pulse velocity, $v$.

In figure 5(h), we have plotted the interaction time versus the velocity of the RIP in the dispersion (red curve) and dispersionless (blue curve) case. Neglecting dispersion, the interaction time tends to infinity as the velocity of the RIP approaches the trapping case. We can interpret this divergence as a (meta)stable state where the photon is trapped inside the pulse. An analytical estimate for this trapping time is given, for the axial geodesic, by the formula $t_{\rm trap} = \frac{2}{c}\int_0^r \frac{n\mathrm{d}\xi}{1-n(\xi)v/c}$, where $r$ represents the longitudinal extension of the RIP. In the dispersionless case $t_{\rm trap}$ diverges, whereas in the dispersive case it is always finite.

## 5. Horizon in optics

In this section, we provide a definition for the horizons from the optical point of view, in the dispersionless case. For the sake of definiteness, we focus on the 'white hole' horizon, but similar considerations hold true for the 'black hole' horizon. We work in the laboratory frame, where the pulse is moving in the $x$-direction, with velocity $v$. The situation is depicted in figure 6(a).

Recall that the ergosphere is defined as the set of points where the velocity of light is the same as the velocity of the pulse, which means that $n(X) = c/v$ for all points $X$ on the ergosphere. In particular, it follows that a light ray reaching the ergosphere, for example in $P$, will not enter the ball if it is moving in the $x$-direction. However, if it is directed along the NW–SE direction (for example toward the centre), then it will cross over the ergosphere, thus entering the ball. This is because it 'sees' the surface move more slowly in such a direction: indeed, note that a plane forming an angle $\theta$ w.r.t. $x$ and moving with velocity $v$ in the $x$-direction appears to move with velocity $u = v\sin\theta < c/n(P)$ along its normal direction, see figure 6(b).

Therefore, only a single point on the ergosphere, namely the axial point $x_-$, behaves as a true white hole horizon. In order to determine whether a full event horizon extends beyond

$x_-$, we impose the condition $u = c/n(Q)$ on some point internal to the ergosphere (where $n(Q) > n(P) = c/v$), which then gives

$$v \sin\theta(Q) = c/n(Q). \tag{20}$$

Now, suppose that the horizon is described by a surface $\rho = h(x - vt)$, where $\rho$ is the radial coordinate. Then

$$\tan\theta(Q) = \frac{\mathrm{d}h}{\mathrm{d}x}(Q). \tag{21}$$

Note that equations (20) and (21) are indeed satisfied by the axial point $x_-$ (for which equation (21) gives $\theta = 90^\circ$). A simple manipulation gives

$$\frac{\mathrm{d}h}{\mathrm{d}x} = \pm\frac{c}{\sqrt{v^2n^2 - c^2}}. \tag{22}$$

Finally, in the comoving frame, using the coordinates $(x', \rho)$, the horizon equation is

$$\frac{\mathrm{d}h}{\mathrm{d}x'} = \pm\frac{\sqrt{c^2 - v^2}}{\sqrt{v^2n^2 - c^2}}. \tag{23}$$

The same equation can be obtained in the following way. It is a common strategy to parameterize the horizon by means of a level set function $F$ such that $F = 0$ on the horizon; the light-like condition for the event horizon is $g^{\mu\nu}(\partial_\mu F)(\partial_\nu F) = 0$. In our case, there are two further requirements: axial symmetry and that the horizon is stationary (i.e. $\partial_{t'}F$=0). Then, in the RIP frame the condition that imposes the normal to the event horizon to be light-like is

$$\gamma^2\left(1 - n^2(x', \rho)\frac{v^2}{c^2}\right)(\partial_{x'}F)^2 + (\partial_\rho F)^2 = 0. \tag{24}$$

In the static case, $\partial_\rho F = 0$, and then from (24) we deduce that the horizon consists of two infinite extended planes, orthogonal to the $x$-axis, located at the solutions $x'_\pm$ of $1 - n^2(x')\frac{v^2}{c^2} = 0$, as described in [17]. In the non-static case, it is evident that the horizon has to be contained within the ergosurface, because it is necessary that $1 - n^2(x, \rho)v^2/c^2 \leqslant 0$. Moreover (at least locally, due to the implicit function theorem), we assume that $F(x', \rho) = 0 \Leftrightarrow \rho - h(x') = 0$, i.e. $F(x', \rho) = \rho - h(x')$. Then, equation (24) becomes $g^{11}(\frac{\mathrm{d}h}{\mathrm{d}x'})^2 + g^{22} = 0$. As a consequence, we obtain $\frac{\mathrm{d}h}{\mathrm{d}x'} = \pm 1/\sqrt{-g^{11}}$, which explicitly corresponds to (23).

According to equations (20) and (21), as described above, the points $x_-$ and $x_+$ for $\rho = 0$ belong to the event horizons, which then represent initial points for the ordinary differential equation (23). Allowed solutions should start from the aforementioned points and remain inside the ergosurface. According to numerical evaluations, carried out for $\eta = 1 - 10^{-4}$, in the range of interest for our assumption that the RIP represents a small perturbation with respect to the refractive index value in the absence of the RIP, the RIP exhibits a somewhat odd behaviour in the sense that the solution does not extend beyond $x_-$ and $x_+$.

Physically, a light ray passing through a point lying outside the ergoregion can travel in either direction (toward the RIP, or away from it). Such a ray is not 'trapped', and therefore such a point cannot belong to an event horizon.

Figure 7 shows the solutions to equation (23) for the case $\eta = 0.1$. The dashed line shows the ergosurface predicted by equation (9) and the solid lines are solutions to equation (23) for different initial conditions. These curves represent light-like surfaces passing through points inside the ergosphere (in the RIP frame). The different null hypersurfaces that pass near $x_+$

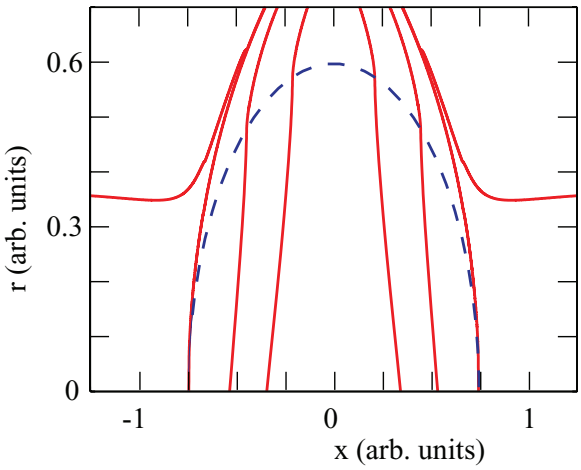


**Figure 7.** Solid lines: real part of the solutions to equation (23). Dashed line: the ergosphere predicted by equation (9). The parameters are $n_0 = 1.45$, $\eta = 0.1$ and $v = c/1.52$.

(or $x_-$) cross the ergosphere at a point that is progressively closer to $x_+$ (or $x_-$). This is numerical evidence of the fact that a hypothetical event horizon cannot extend beyond the points $x_+$ and $x_-$. As can be seen, the solutions that pass through $x_+$ and $x_-$ are tangent to the ergosurface and always remain *outside* the latter so that the horizon effectively reduces to a point. We note that strictly speaking even though these points behave like points of a trapping horizon, as shown for example in figure 3, it is of course not possible to define them as event horizons in the sense of a light-like hypersurface. One may wonder whether a 'trapping point' is expected to still emit Hawking-like radiation and, if so, with which features. In particular, can we rely on some arguments in order to support the idea that there is a pair-creation process that, moreover, still shares common features with the Hawking effect? We show in a forthcoming work that the answer is affirmative [18]. Points where the ergosurface becomes light-like, beyond their properties to be trapping points, which behave as standard horizons, share the further property of involving production of particles with a thermal spectrum, again like the case of standard (non-degenerate) horizons.

## 6. Conclusions

We have derived the effective metric associated with an RIP in a nonlinear Kerr medium. Such a metric simulates the effect on light rays of the presence of a dielectric perturbation in a sample of an isotropic $\chi^{(3)}$ dielectric material. Then, we have investigated the possibility for an ergoregion to arise, and the behaviour of geodesics by means of numerical simulations, also taking into account the presence of dispersion. Finally, we have provided an equation for the event horizon that highlights a rather peculiar geometry, as it appears that the solutions may reduce to a single point. Numerical evaluation in the range of interest confirms the former conclusion. Still, the two special points $x_-$ and $x_+$ of the ergosurface exhibit trapping properties like those of a standard trapping horizon from a classical point of view.

## Appendix. A remark on the extraordinary metric

We show that, under reasonable approximations, the extraordinary metric can be recast in the Gordon form. We work in a reference frame at rest w.r.t. the medium (the laboratory frame). Consider a background field $E$ that, in the laboratory frame, has polarization vector orthogonal to its direction of propagation $x$. We can choose Cartesian coordinates $(t, x, y, z)$ so that $l^\mu = (0, l_x = 0, l_y = 0, l_z = 1)$. The line element for the extraordinary rays takes the form

$$\mathrm{d}s^2_{(-)} = \frac{c^2}{\tilde{n}^2}\mathrm{d}t^2 - \mathrm{d}x^2 - \mathrm{d}y^2 - \left(1 - \frac{\xi}{1+\xi}\right)\mathrm{d}z^2. \tag{A.1}$$

Note that the factor in front of $\mathrm{d}z^2$ cannot vanish. Moreover, $\xi \ll 1$ (see also [17]). Then, we can safely keep only the leading order term in the $z$ part of the metric so that, in so doing, the extraordinary metric reduces to

$$\mathrm{d}s^2_{(-)} = \frac{c^2}{\tilde{n}^2}\mathrm{d}t^2 - \mathrm{d}x^2 - \mathrm{d}y^2 - \mathrm{d}z^2. \tag{A.2}$$

Under this approximation, the effective metric for extraordinary rays has again the same form as the Gordon one, with an effective refractive index

$$\tilde{n} = \sqrt{\mu_\mathrm{r}\varepsilon_\mathrm{r}(1+\xi)} = n_0 + \frac{3}{2}\frac{\sqrt{\mu_r}\chi^{(3)}E^2}{(1+\chi^{(1)})^{1/2}} = n_0 + 3\delta n, \tag{A.3}$$

to be compared to the refractive index for the ordinary rays, which is

$$n = \sqrt{\mu_\mathrm{r}\varepsilon_\mathrm{r}} = n_0 + \frac{1}{2}\frac{\sqrt{\mu_\mathrm{r}}\chi^{(3)}E^2}{(1+\chi^{(1)})^{1/2}} = n_0 + \delta n. \tag{A.4}$$

Here, $n_0$ is the refractive index of the medium when we disregard nonlinear effects, i.e.

$$n_0 = \sqrt{\mu_\mathrm{r}\varepsilon_\mathrm{r}} = \sqrt{\mu_\mathrm{r}\left(1+\chi^{(1)}\right)}. \tag{A.5}$$

Then, the extraordinary rays 'feel' a disturbance of the refractive index three times stronger than the ordinary ones. The same conclusion can be also achieved in the context of Hawking radiation production by an RIP [18]. Indeed, it can be shown that the differential equation that defines the extraordinary field modes is well approximated by the same equation as for the ordinary ones, apart from an effective RIP three times larger.

## References


[1] Gordon W 1923 Zur Lichtfortpflanzung nach der relativitätstheorie *Ann. Phys.* **377** 421–56

[2] Leonhardt U and Piwnicki P 1999 Optics of nonuniformly moving media *Phys. Rev.* A **60** 4301–12

[3] Leonhardt U and Piwnicki P 2000 Relativistic effects of light in moving media with extremely low group velocity *Phys. Rev. Lett.* **84** 822–5

[4] Schützhold R, Plunien G and Soff G 2002 Dielectric black hole analogs *Phys. Rev. Lett.* **88** 061101

[5] Brevik I H and Halnes G 2001 Light rays at optical black holes in moving media *Phys. Rev.* D **65** 024005

[6] De Lorenci V A and Klippert R 2002 Analogue gravity from electrodynamics in nonlinear media *Phys. Rev.* D **65** 064027

[7] De Lorenci V A and Souza M A 2001 Electromagnetic wave propagation inside a material medium: an effective geometry interpretation *Phys. Lett.* B **512** 417–22

[8] Novello M and Salim J M 2001 Effective electromagnetic geometry *Phys. Rev.* D **63** 083511

[9] Marklund M, Anderson D, Cattani F, Lisak M and Lundgren L 2002 Fermat's principle and the variational analysis of an optical model for light propagation exhibiting a critical radius *Am. J. Phys.* **70** 680–3
[10] De Lorenci V A, Klippert R and Obukhov Yu N 2003 On optical black holes in moving dielectrics *Phys. Rev.* D **68** 061502
[11] Novello M, Perez B, Santiago E, Salim J, De Lorenci V and Klippert R 2003 Analog black holes in flowing dielectrics *Class. Quantum Gravity* **20** 859–72
[12] Novello M, Perez B and Santiago E 2003 Effective geometry *AIP Conf. Proc.* **668** 288–300
[13] Unruh W G and Schützhold R 2003 On slow light as a black hole analogue *Phys. Rev.* D **68** 024008
[14] Schutzhold R and Unruh W G 2005 Hawking radiation in an electro-magnetic waveguide? *Phys. Rev. Lett.* **95** 031301
[15] Philbin T G, Kuklewicz C, Robertson S, Hill S, Konig F and Leonhardt U 2008 Fiber-optical analog of the event horizon *Science* **319** 1367
[16] Faccio D, Cacciatori S, Gorini V, Sala V G, Averchi A, Lotti A, Kolesik M and Moloney J V 2010 Analogue gravity and ultrashort laser pulse filamentation *Europhys. Lett.* **89** 34004
[17] Belgiorno F, Cacciatori S L, Gorini V, Ortenzi G, Rizzi L and Faccio D 2010 Dielectric black holes induced by a refractive index perturbation and the Hawking effect *Phys. Rev.* D submitted (arXiv:1003.4150)
[18] Belgiorno F, Cacciatori S L, Gorini V, Ortenzi G, Rizzi L and Faccio D. 2010 in preparation
[19] Robertson S and Leonhardt U 2010 Frequency shifting at fiber-optical event horizons: the effect of Raman deceleration *Phys. Rev.* A **81** 063835
[20] Wald R M 1984 *General Relativity* (Chicago, IL: University of Chicago Press)
[21] Visser M 1998 *Class. Quantum Gravity* **15** 1767–91